Geophysical Research Letters

Supporting Information for

Arctic Tropospheric Ozone Trends

K. S. Law[1], J. Liengaard Hjorth[2], J. B. Pernov[2,3], C. H. Whaley[4], H. Skov[2], M. Collaud Coen[5], J. Langner[6], S. R. Arnold[7], D. Tarasick[8], J. Christensen[2], M. Deushi[9], P. Effertz[10,14], G. Faluvegi[11,12], M. Gauss[13], U. Im[2], N. Oshima[9], I. Petropavlovskikh[10,14], D. Plummer[4], K. Tsigaridis[11,12], S. Tsyro[13], S. Solberg[15] and S.T. Turnock[16,7]

[1]Sorbonne Université, LATMOS/IPSL, UVSQ, CNRS, Paris, France
[2]Department of Environmental Science, Interdisciplinary Centre for Climate Change, Aarhus University, Frederiksborgvej 4000, Roskilde, Denmark
[3]Extreme Environments Research Laboratory, École Polytechnique fédérale de Lausanne, 1951 Sion, Switzerland
[4]Canadian Centre for Climate modeling and analysis, Environment and Climate Change Canada, Victoria, BC, Canada
[5]Federal Office of Meteorology and Climatology, MeteoSwiss, Payerne, Switzerland
[6]Swedish Meteorological and Hydrological Institute, Norrköping, Sweden
[7]Institute of Climate and Atmospheric Science, School of Earth and Environment, University of Leeds, Leeds, United Kingdom
[8]Air Quality Research Division, Environment and Climate Change Canada, Toronto, ON, Canada
[9]Meteorological Research Institute, Japan Meteorological Agency, Tsukuba, Japan
[10]Cooperative Institute for Research in Environmental Sciences (CIRES), University of Colorado, Boulder, CO, USA.
[11]NASA Goddard Institute for Space Studies, New York, NY, USA
[12]Center for Climate Systems Research, Columbia University; New York, USA
[13]Norwegian Meteorological Institute, Oslo, Norway
[14]National Oceanic and Atmospheric Administration (NOAA) ESRL Global Monitoring Laboratory, Boulder, CO, USA.
[15]Norwegian Institute for Air Research (NILU), Kjeller, Norway.
[16]Met Office Hadley Centre, Exeter, UK

Contents of this file

Introduction

The supporting information gives details about surface and ozonesonde data coverage (Text S1, Figs. S1 and S2), the trend analysis method (Text S2), and the models (Text S3) used in this study, and discusses trends of tropospheric ozone (O_3) precursors in the Arctic (Text S4). Additional figures show O_3 trends at Arctic locations not shown in the main text, and trends over different time periods for both the observations and models (Figs. S3-S9). Trends in surface carbon monoxide (CO) (Fig. S10), and in low springtime O_3 concentrations at Canadian Arctic

sites (Fig. S11) are also shown. Tables S1 and S2 provide additional details about the models and surface annual O_3 trends, respectively. See Fig. 1 in main text for measurement site locations.

Text S1. Data coverage

To ensure proper statistical representation of the data coverage thresholds at least 50% of available data is required for the calculation of monthly and annual trends. Data coverage for the surface sites is shown in Fig. S1. It is also verified that at least one complete year of data is available at the beginning and end of the time series, since incomplete years at the beginning and end of a time series can have a larger influence on trend analysis results (Collaud Coen et al., 2020). Esrange has full data coverage, with less than five months having coverage lower than 50%. Pallas, Summit, Tustervatn and Zeppelin have one to three periods of 1-2 years without data that do not preclude long-term trend analysis, although it should be noted that the Summit record only started in June 2000. Alert and Villum have a high monthly data coverage but suffer from missing data over a 4-5 year period in the middle of the time series. For Alert, there are two missing periods throughout the time series. For Villum there is only one missing period although the period 1996-2002 suffers from poor data coverage. Therefore, trends at Villum and Alert can be considered as valid but should be interpreted with caution (Collaud Coen et al., 2020).

Ozonesondes were launched at least once per week at the six Arctic stations used in this analysis. There are periods with up to three soundings a week, mostly in winter and spring (Fig. S2). Periods without measurements do not exceed 1 month except at Eureka, where there are five periods with missing data of three to eight months mostly in spring (2000, 2003, 2005, 2006, and 2016) and a 3-month period missing in 2006 at Sodankyla. The mean yearly number of soundings varies between 38 (Resolute) and 90 (Ny Ålesund). At Alert and Sodankyla a lower number of soundings were performed in 2016-2020. A visual inspection of the O_3 time series at the 20 pressure levels used in this analysis does not show evidence for any rupture apart from at the 4 lowest levels before 1995 at Eureka, potentially resulting in lower O_3 concentrations.

Text S2. Trend analysis methodology

Long-term trend determination needs to be applied to homogeneous time series in order to analyze real variations or changes in the observations as opposed to artifacts. For the surface O_3 concentrations, while data is taken from quality-controlled repositories, this does not take into account technical changes such as modification or changes in instrumentation, station position, changes to calibration procedures or instrumental drifts. Visual inspection allowed detection of potential ruptures in the time series.

Trends in surface O_3 concentrations at different sites are determined using the non-parametric Mann-Kendall test and Sen's slope methodology (Theil, 1950; Sen, 1968), and calculated using daily medians of the O_3 volume mixing ratios using hourly observations. These tests require the data to be serially independent and homogeneously distributed. However, the O_3 measurements are significantly lag-1 auto-correlated and exhibit high amounts of seasonality. Therefore, the data is prewhitened to remove the lag-1 autocorrelation. The seasonal Mann-Kendall test is applied to address the seasonality present in the data (Hirsch et al., 1982) using the Matlab version (Collaud Coen and Vogt, 2021) of the 3PW algorithm from Collaud Coen et al. (2020).

The 3PW method uses two prewhitening methods prior to testing for statistical significance. The first method from Kulkarni and von Storch (1995) simply removes the lag-1 autocorrelation (referred to as PW). This method has a low rate of false positives but lowers the power of the Mann-Kendall test. The second prewhitening method from Yue and Wang (2002), detrends the data before prewhitening (referred to as TFPW-Y). This method returns the power of the Mann-Kendall test although it increases the rate of false positives. Trends must be statistically significant using both methods to be considered significant in the 3PW algorithm. If a significant trend is present, then the slope is calculated using the variance corrected trend free prewhitening (VCTFPW) method from Wang et al. (2015), which gives an unbiased estimate of the Theil Sen slope. This method maximizes the advantages of these prewhitening methods and minimizes their disadvantages. We use the seasonal Mann-Kendall test on a monthly temporal segmentation (i.e., a trend analysis is performed on each value in a respective month over the period analyzed). For the O_3 soundings weekly resolution is applied since regular daily measurements are not available. Relative monthly trends (% per year) for the 20 pressure levels of the ozonesonde data are calculated as absolute monthly trends divided by monthly median concentrations x 100 %. Statistically significant (ss) trends are determined at the 90^{th} and 95^{th} % confidence levels (CLs). The Theil-Sen estimator is the median of all possible pairwise slopes. Upper CL and lower CL, on the 95^{th} % CL, contain the middle 95% of the pairwise slopes, which are normally distributed (Gilbert, 1987). To test the robustness of the results, trends are also compared for different periods of available records (1993-2019, 1993-2013, 1999-2019), and comparison with the model results (1995-2015). Monthly medians are used to compare model results with the observations since higher temporal resolution results are not available from the models. In all cases, model results are averaged to produce multi-model median (MMM) results.

For trends in the yearly median, a simple Mann-Kendall test and Theil Sen Slope without prewhitening are employed, using the MAKESENS application (Salmi et al., 2002), since there is no seasonality present, and the data are not autocorrelated. The minimum requirement for including observation series in this evaluation is data available from 1996 to 2018 in order to have comparable trends. Nearly all of the stations have years with less than 50% data coverage which are not included in the calculations of the annual trends. Relative trends are given as percentages of median concentrations.

Text S3. Models

Four global chemistry-climate (CMAM, GISS-E2.1, MRI-ESM2, UKESM1) and two chemistry-transport (DEHM, EMEP MSC-W) models were run using the same (ECLIPSEv6b) anthropogenic emissions for 1990 (1995 for GISS model) to 2015 as part of the Arctic Monitoring and Assessment Programme (AMAP) assessment (AMAP, 2021). They were run with different biogenic emissions and meteorology and nudged using different reanalysis products (see Table S1). The models also vary in their representation of the stratosphere with only a subset of having a fully simulated stratosphere. CMAM, MRI-ESM2, GISS-E2.1, and UKESM1 contain relatively complete stratospheric O_3 chemistry (involving nitrogen oxides (NO_x), chlorine and bromine chemistry), while the other models have no stratospheric chemistry (DEHM, EMEP MSC-W). Model results from 1995-2015 are used in this study.

Present-day model simulations for 2014-2015, including the models contributing to this study, were evaluated first against a limited set of tropospheric Arctic O_3 observations (Whaley et al., 2022), and also in more detail, including tropospheric Arctic O_3 seasonal cycles, in our companion paper Whaley et al. (2023). These evaluations show large variability in model performance. The MMMs capture surface Arctic O_3 observations quite well, except for low concentrations observed during high Arctic polar spring (Whaley et al., 2023). Most atmospheric models, including all of the models in this study, do not yet contain Arctic tropospheric halogen chemistry, and thus cannot simulate the surface-level bromine and iodine-driven O_3 depletion events that occur during spring at some Arctic locations (Whaley et al., 2023). Model performance in the free troposphere is better (within +/- 10%) compared to satellite, aircraft and ozonesonde data, but upper tropospheric O_3 is overestimated (Whaley et al., 2022, 2023).

Text S4. Trends in tropospheric Arctic O_3 precursors

To understand Arctic tropospheric O_3 trends, it is important to understand trends in O_3 precursors as well as other factors such as changing transport patterns. O_3 precursors include methane (CH_4), CO, NO_x and non-methane volatile organic compounds (NMVOCs). While, as pointed out in the main text, precursor trends over Northern Hemisphere (NH) mid-latitude emission regions are likely contributing to changes in Arctic tropospheric O_3, it is also useful to examine precursor trends in the Arctic, when long-term measurements are available, and to evaluate MMM trends. The contribution of different sources, including precursor emissions, and sinks of Arctic O_3 is discussed in Whaley et al. (2023) and references therein.

Arctic CH_4 at the surface rose from 1.75 ppmv in 1984 to 1.95 ppmv in 2020 (AMAP, 2021). The increasing trend was interrupted by a plateau between 2000 and 2005 that accelerated after 2015 based on data from Pallas, Zeppelin and Utqiaġvik (formerly known as Barrow). AMAP (2021) derived an ss (95^{th} % CL) observed annual trend of +2.29+/-0.55 ppbv per year, whereas modeled CH_4, which was prescribed, had an annual trend of +2.79 ppbv per year, ss only at 90^{th} % CL. Thus, modeled and measured trends are reasonably comparable. Around 40% of Arctic O_3 response to precursor emission changes may be due to increasing CH_4 (AMAP, 2015).

Mackie et al. (2016) showed that CO decreased from 1989-2012 at Utqiaġvik with the largest ss decreases in winter and spring attributed to decreasing anthropogenic CO emissions in Europe and North America. Figure S10 compares seasonal CO trends from observations and MMM results at the few sites with long time series (Alert, Utqiaġvik and Zeppelin). These trend calculations are based on monthly averages, applying the 3PW algorithm, as discussed in 2.3 and S2, for periods with available data. MMM results are in general agreement with the observations showing ss negative trends in winter and autumn. However, it can be noted that the models underestimate surface NH CO in winter (Whaley et al, 2023). This discrepancy is larger earlier in the time series, while the models agree better with observed CO later in the time series (not shown).

There are no reported trends in NO_x or NMVOCs in the Arctic due to a lack of long-term measurements (AMAP, 2021). In general, observed NMVOC concentrations are low at Arctic sites monitoring background air masses, and away from local sources (Pernov et al. 2021). Thus,

local NMVOC photo-oxidation only has limited effect on Arctic tropospheric O_3 as discussed by Helmig et al. (2014) and Gautrois et al. (2003). However, long-range transport of air masses, influenced by mid-latitude anthropogenic and natural NMVOC emissions, can influence Arctic tropospheric O_3 (Whaley et al., 2023). NO_x concentrations are also generally low in the background Arctic troposphere (Whaley et al., 2023), but can be elevated near local sources, for example due to shipping emissions (e.g. Marelle et al., 2016). Also, long-range transport of NO_x reservoir species such as peroxy-acetyl nitrate (PAN) or nitric acid can decompose in the warmer spring and summer months producing NO_x (Law et al. (2014) and refs therein). Walker et al. (2012) estimated that more than 50% of O_3 in the Arctic during summer is formed from local PAN decomposition. Whaley et al (2023) showed that MMMs underestimate CO and NO_x throughout the troposphere, but overestimates PAN compared to observed aircraft profiles in the Arctic. Despite these differences, models match observed O_3 profiles in the troposphere, but significantly overestimates O_3 near the tropopause, as noted earlier.

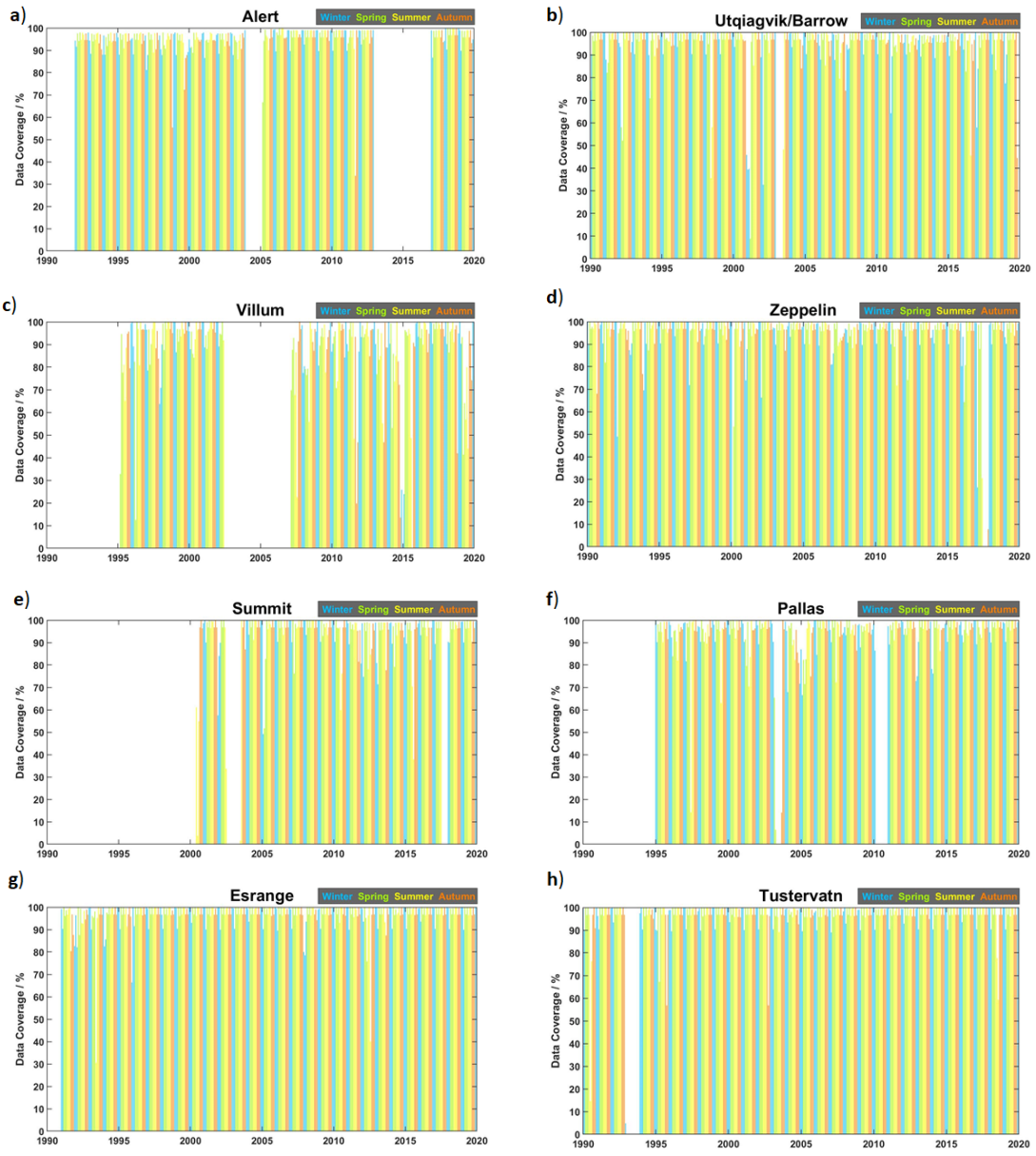

180

181

182 **Figure S1.** *Data coverage for surface O_3 measurements at a) Alert, b) Utqiaġvik, c) Villum, d)*
183 *Zeppelin, e) Summit, f) Pallas, g) Esrange, and h) Tustervatn. Coverage is given as a percentage*
184 *of hours with measurements compared to the total number of hours for each month. Monthly*
185 *coverage is color-coded by the meteorological seasons. See Figure 1 for station locations.*

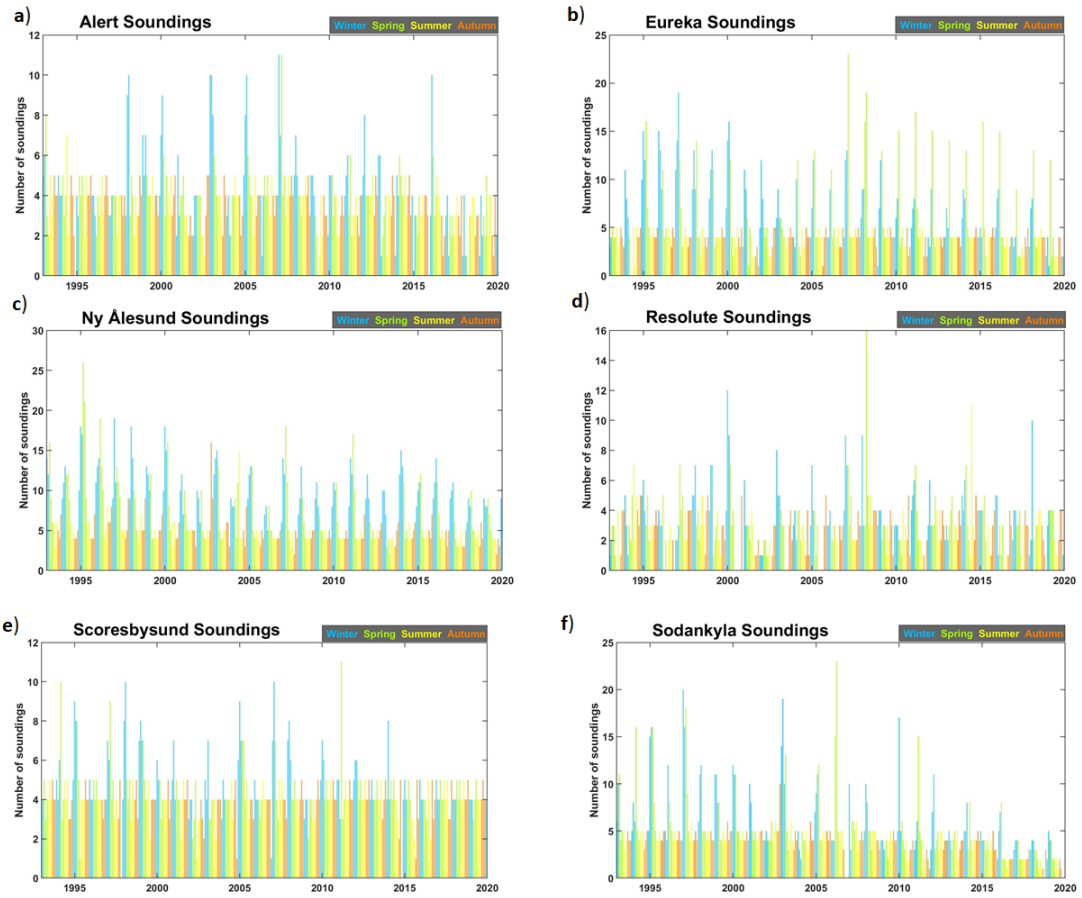

Figure S2. *Ozonesonde data coverage at a) Alert, b) Eureka, c) Ny Alesund, d) Resolute, e) Scoresbysund, and f) Sodankyla. The number of O_3 soundings in each month is shown color-coded by the meteorological seasons. See Figure 1 for station locations.*

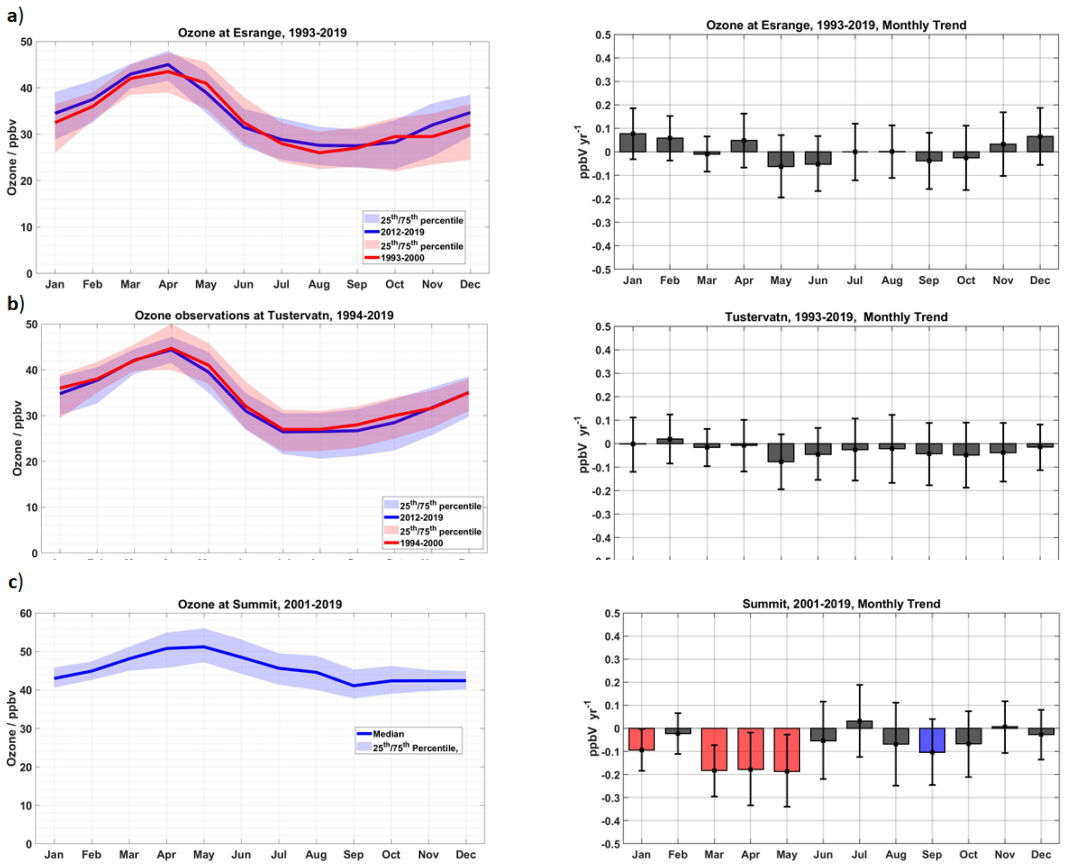

191

192

193 **Figure S3.** *Observed surface O_3 trends and seasonal cycles. Left panels: seasonal cycles of*
194 *monthly median O_3 (ppbv) at a) Esrange, and b) Tustervatn for 1993-2000 (blue lines) vs 2012-*
195 *2019 (red lines), and c) Summit for 2001-2019 only. Shaded areas show upper and lower*
196 *quartiles of hourly values. Right panels: monthly trends over 1993-2019, or for shorter periods*
197 *depending on data availability. Boxes represent the slope of the trend in ppbv per year with red*
198 *boxes significant at 95th% CL, blue boxes at 90th% CL, and black boxes not statistically*
199 *significant. Error bars show 95th% CLs.*

200

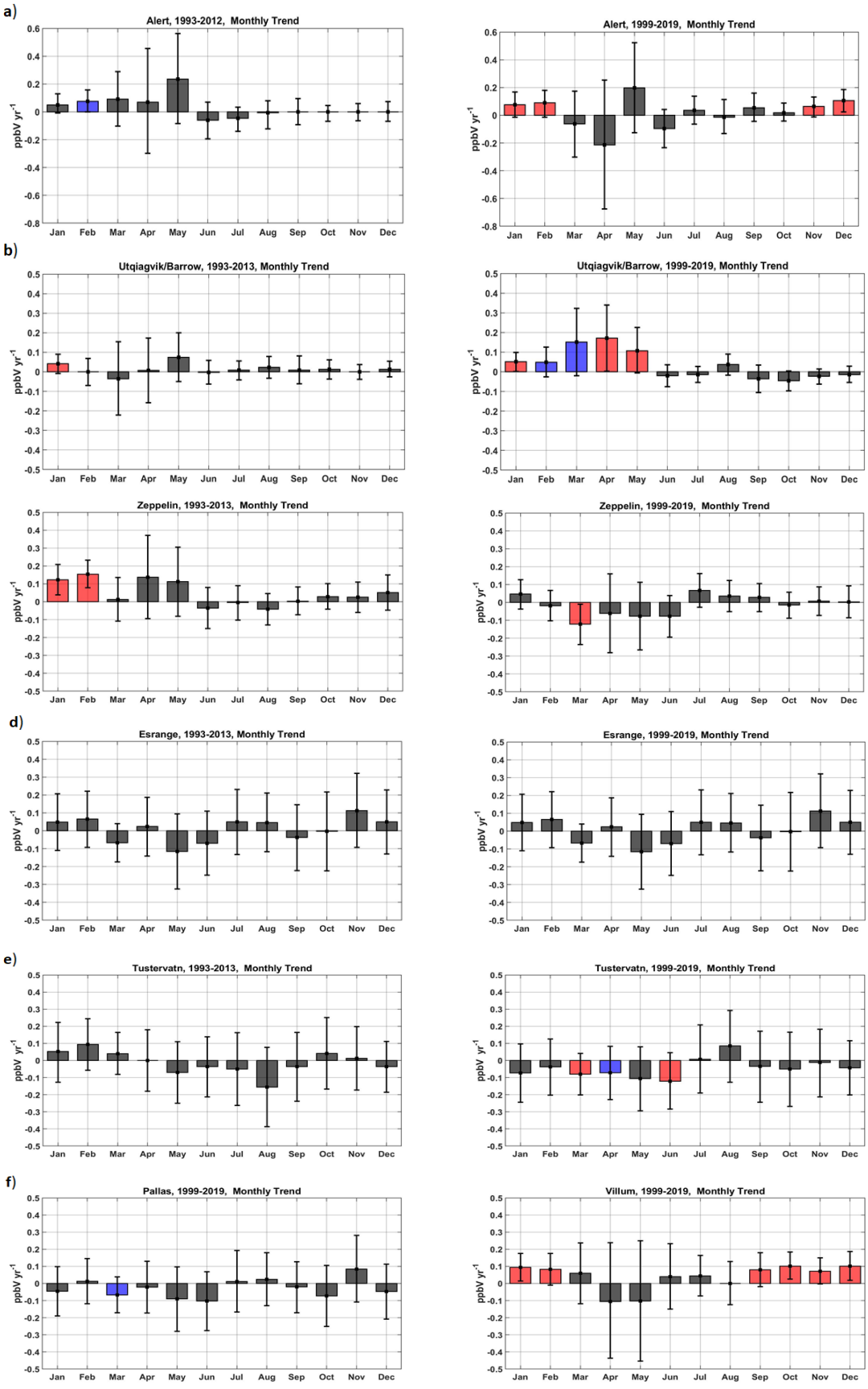
a)
Alert, 1993-2012, Monthly Trend
Alert, 1999-2019, Monthly Trend
b)
Utqiagvik/Barrow, 1993-2013, Monthly Trend
Utqiagvik/Barrow, 1999-2019, Monthly Trend
Zeppelin, 1993-2013, Monthly Trend
Zeppelin, 1999-2019, Monthly Trend
d)
Esrange, 1993-2013, Monthly Trend
Esrange, 1999-2019, Monthly Trend
e)
Tustervatn, 1993-2013, Monthly Trend
Tustervatn, 1999-2019, Monthly Trend
f)
Pallas, 1999-2019, Monthly Trend
Villum, 1999-2019, Monthly Trend
ppbV yr-1
Jan Feb Mar Apr May Jun Jul Aug Sep Oct Nov Dec

201

202

203

Figure S4. *Comparison of observed surface O_3 monthly median trends in ppbv per year for different time periods at a) Alert, b) Utqiaġvik, c) Zeppelin, d) Esrange, e) Tustervatn for 1993-2012 and 1999-2019, depending on data availability, and f) Pallas (left) and Villum (right) for 1999-2019, when good data coverage is available. Box coloring and error bars are the same as Fig. S3 (right panels).*

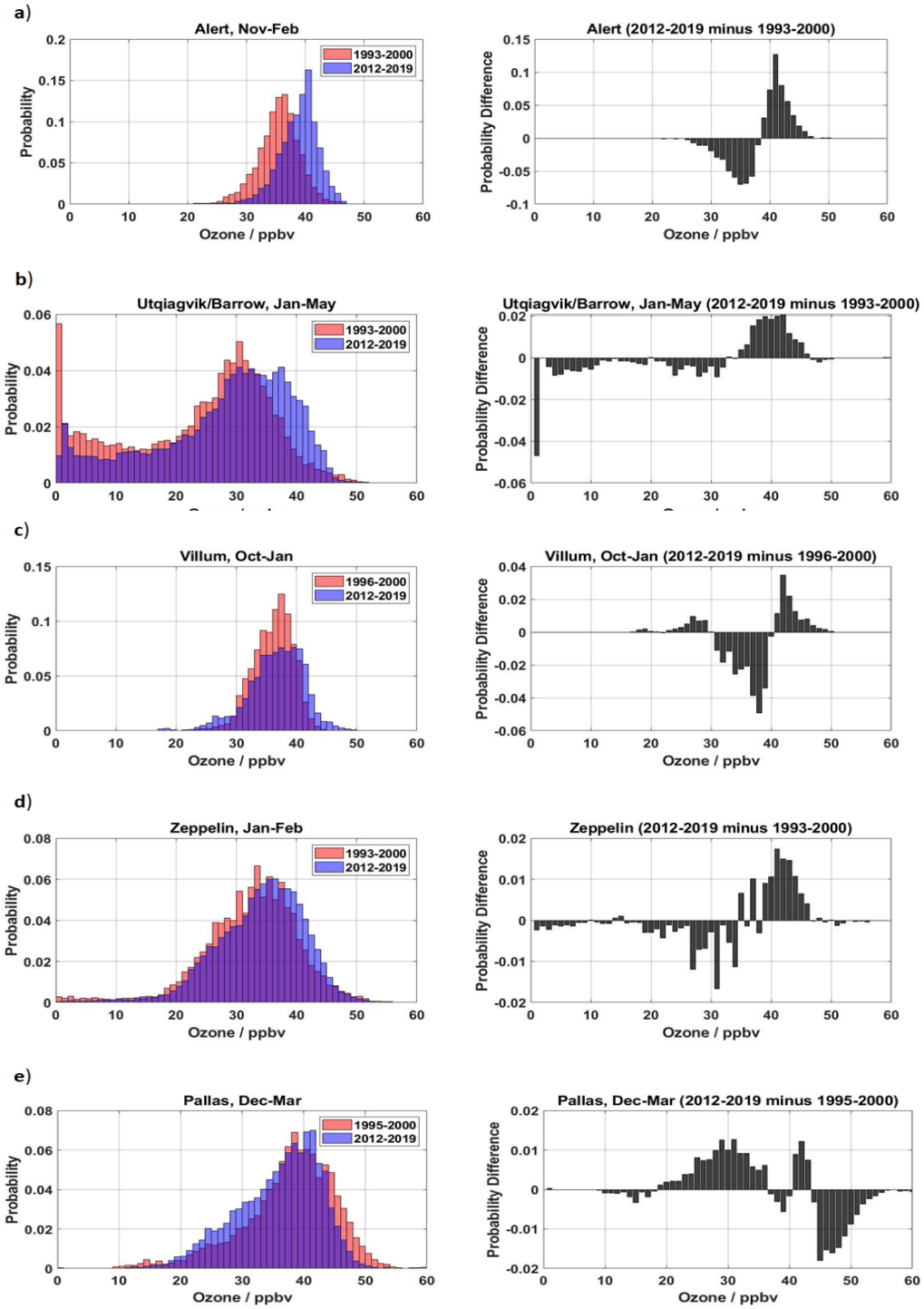

Figure S5. *Changes in probability distributions of surface O_3 concentrations in ppbv between earlier (1993-2000) and later (2012-2019) periods for selected months with statistically significant trends (see Figs. 2 and S3) at a) Alert, b) Utqiaġvik, c) Villum, d) Zeppelin, and e) Pallas. Periods shown vary depending on data availability.*

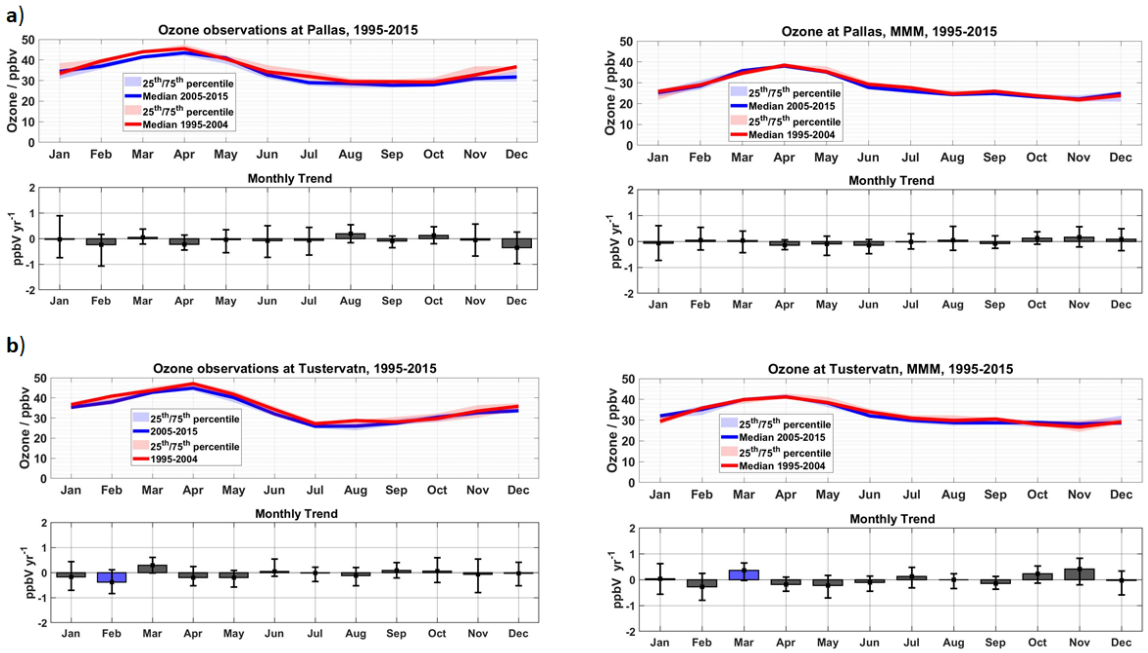

217

218 **Figure S6.** *Comparison of observed (left) and MMM (right) surface O_3 trends and seasonal*
219 *cycles at a) Pallas and b) Tustervatn. Upper panels: seasonal cycles for 1995-2004 (red lines) vs*
220 *2005-2015 (blue lines). Shaded areas show upper and lower quartiles of hourly values*
221 *(observations only). Lower panels: monthly median trends in ppbv per year for 1995-2015. Box*
222 *coloring and error bars are the same as Fig. S3. Shorter periods are shown depending on data*
223 *availability.*

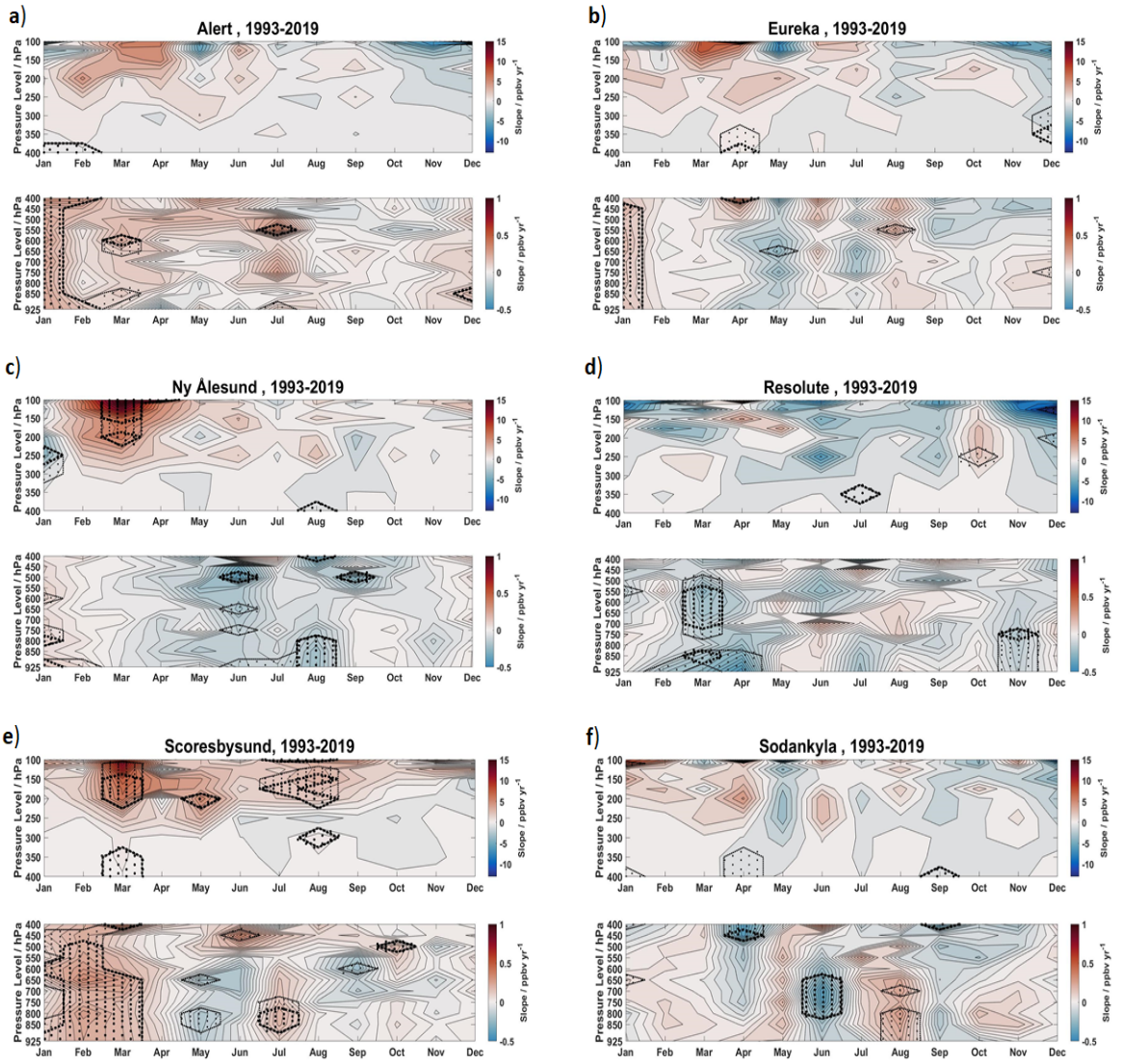

224

225

226 **Figure S7a.** *Absolute vertical trends in observed monthly O_3 for 1993-2019 in ppbv per year at a)*
227 *Alert, b) Eureka, c) Ny Alesund, d) Resolute, e) Scoresbysund and f) Sodankyla. Upper panels:*
228 *upper troposphere and lower stratosphere (400-100 hPa). Lower panels: mid- and lower*
229 *troposphere (925-400 hPa). Note the different color scales. Stippled lines/areas show statistical*
230 *significance at the 90th % CL (smaller marker size) and 95th % CL (larger marker size).*

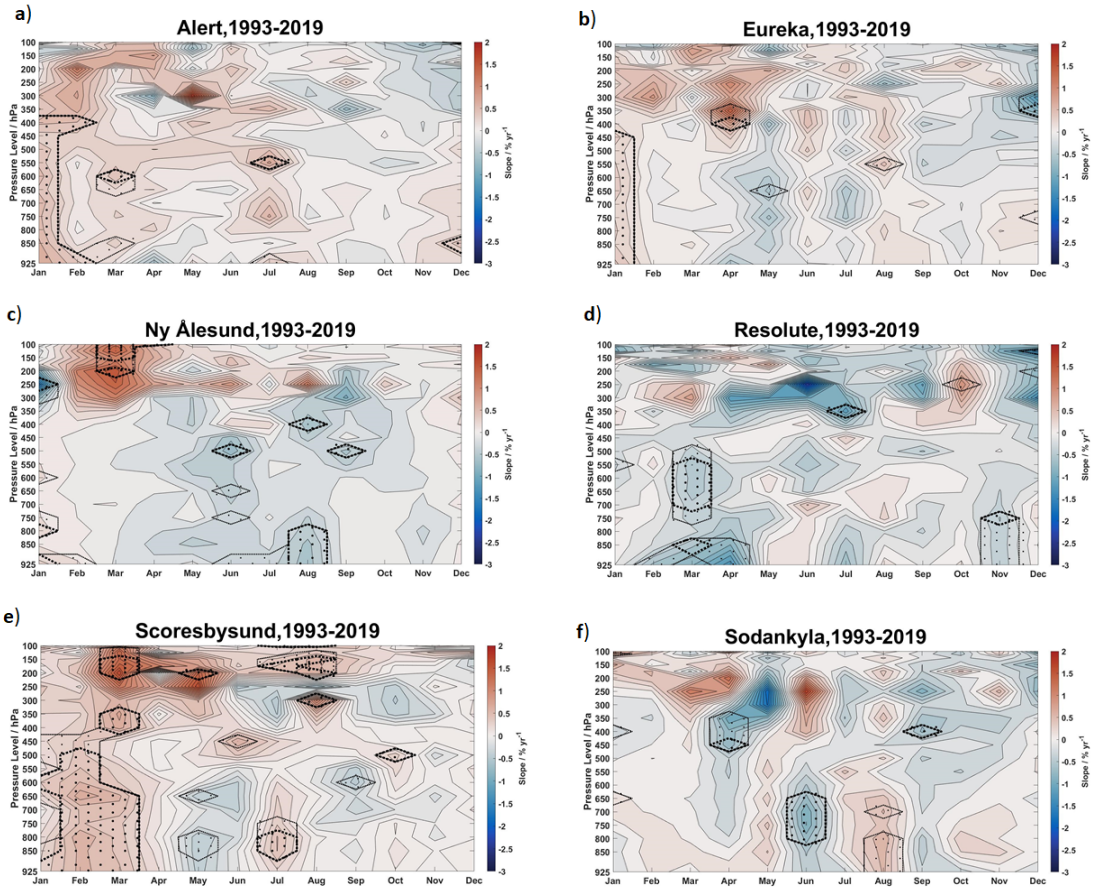

231

232

233

234 **Figure S7b:** *Same as Figure S7a, but vertical trends from 925-100 hPa in observed monthly O_3*

235 *for 1993-2019, relative to monthly median concentrations, in % per year. Shading and symbols*

236 *are the same as Fig S7a.*

237

a)

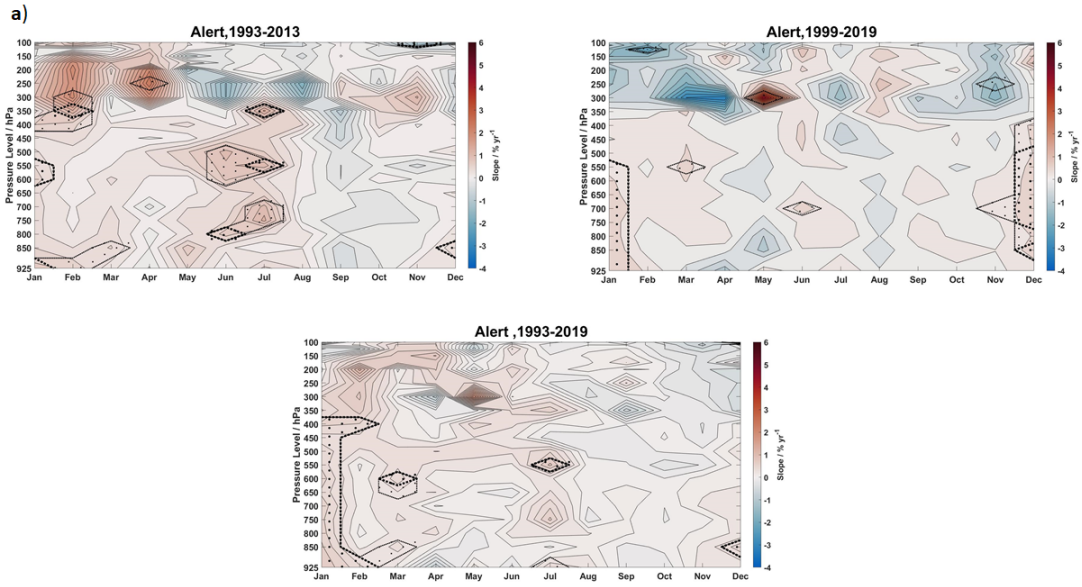

238

b)

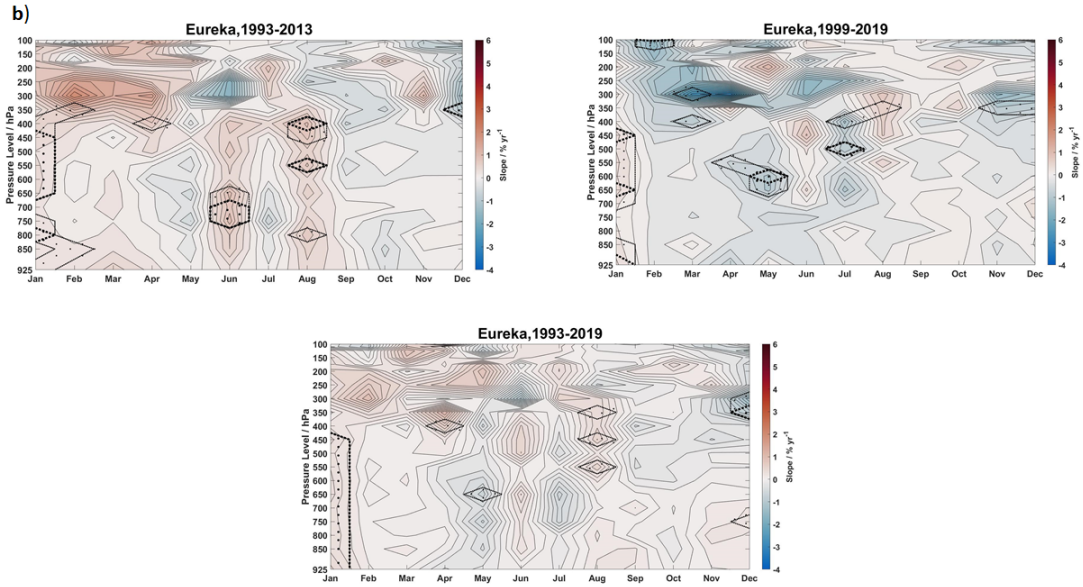

239

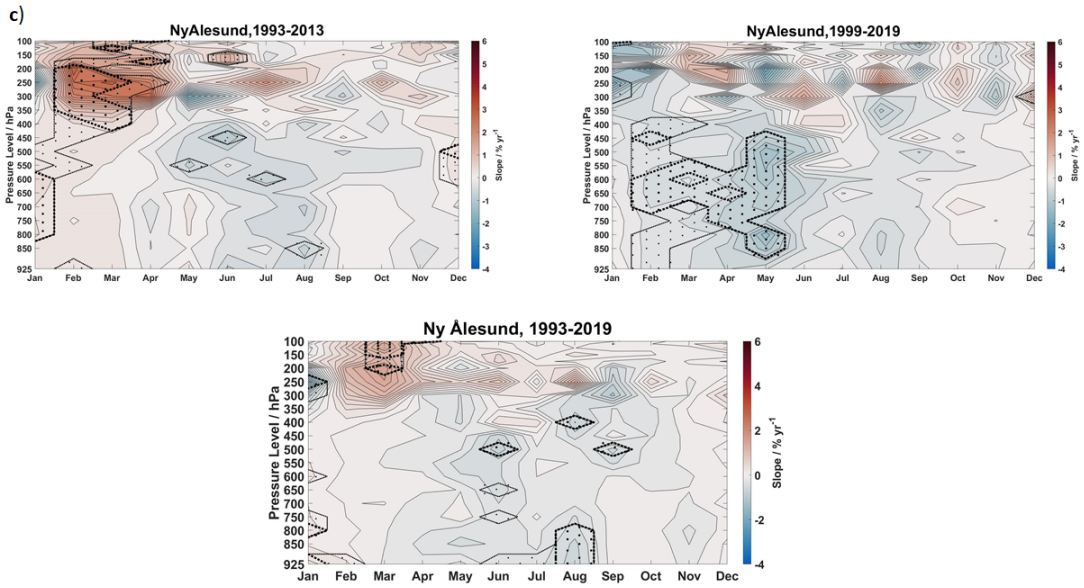
c)
NyAlesund,1993-2013
NyAlesund,1999-2019
Ny Ålesund, 1993-2019
Pressure Level / hPa
Slope / % yr-1
Jan Feb Mar Apr May Jun Jul Aug Sep Oct Nov Dec

240

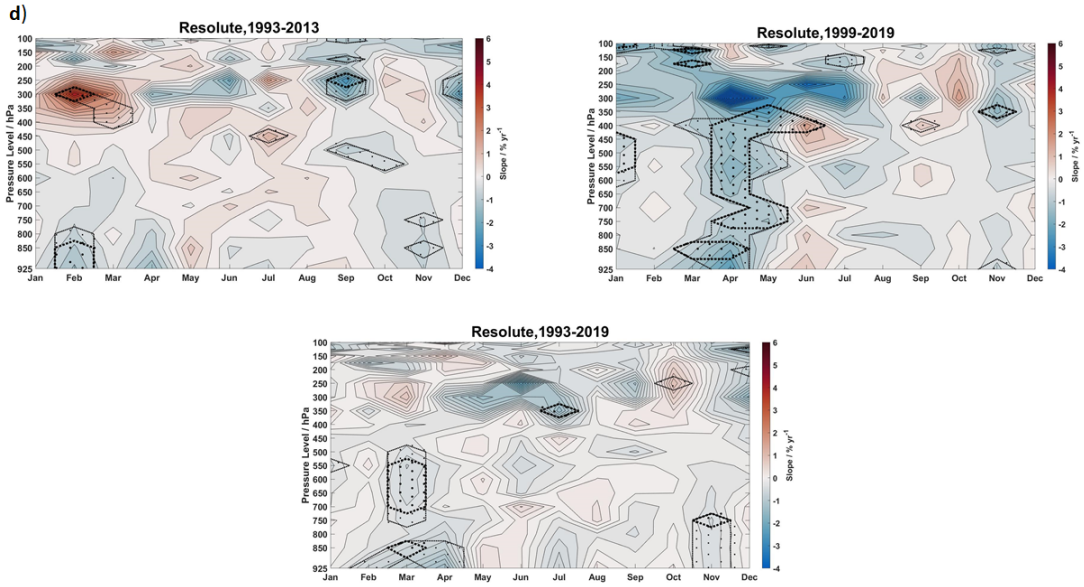
d)
Resolute,1993-2013
Resolute,1999-2019
Resolute,1993-2019
Pressure Level / hPa
Slope / % yr-1
Jan Feb Mar Apr May Jun Jul Aug Sep Oct Nov Dec

241

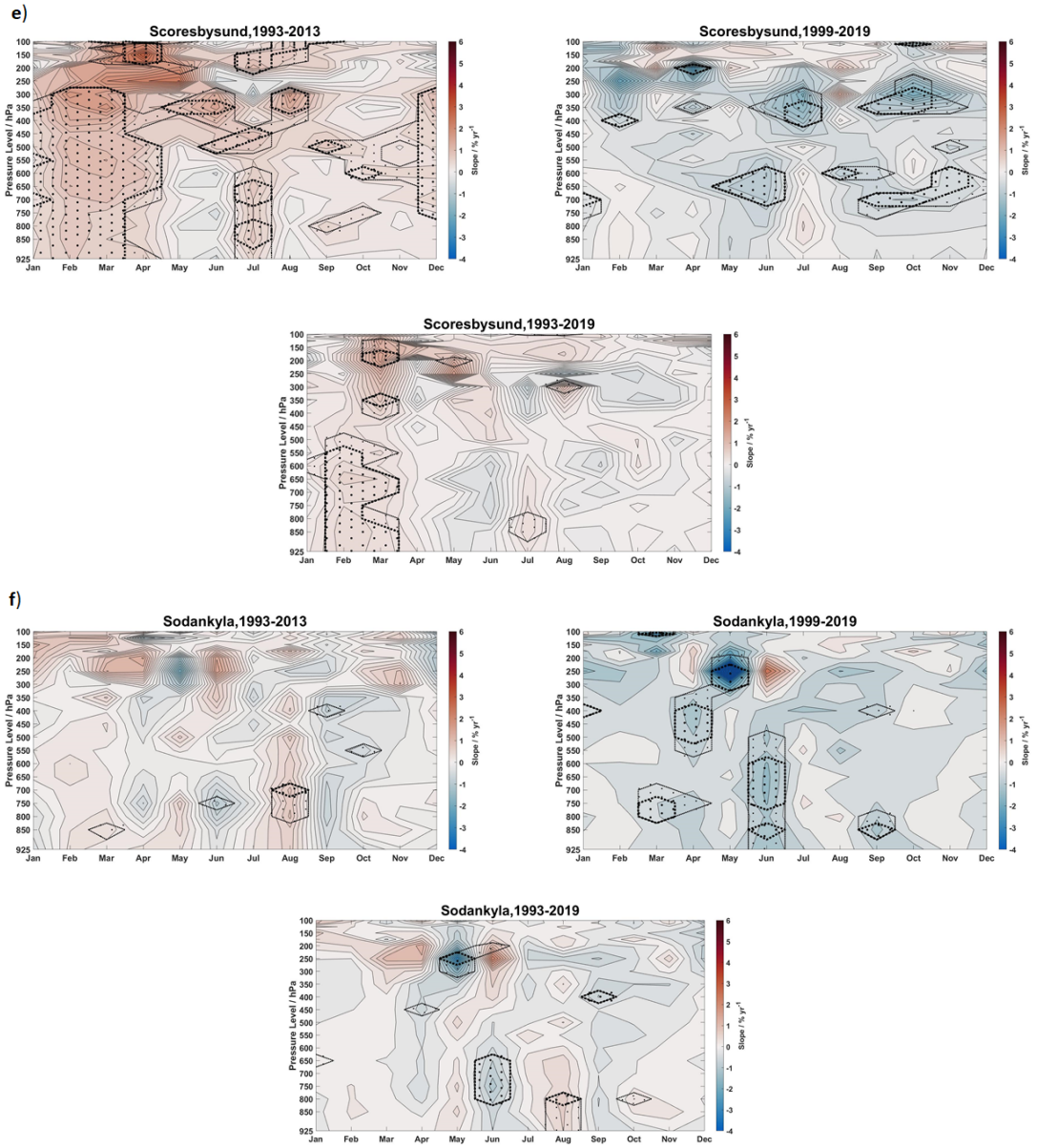

Figure S8. *Vertical trends in observed monthly O_3, relative to monthly median concentrations, in % per year, for different time periods (1993-2013, 1999-2019, and 1993-2019) from 925-100 hPa at a) Alert, b) Eureka, c) Ny Alesund, d) Resolute, e) Scoresbysund, and f) Sodankyla. Shading and symbols are the same as Fig S7a.*

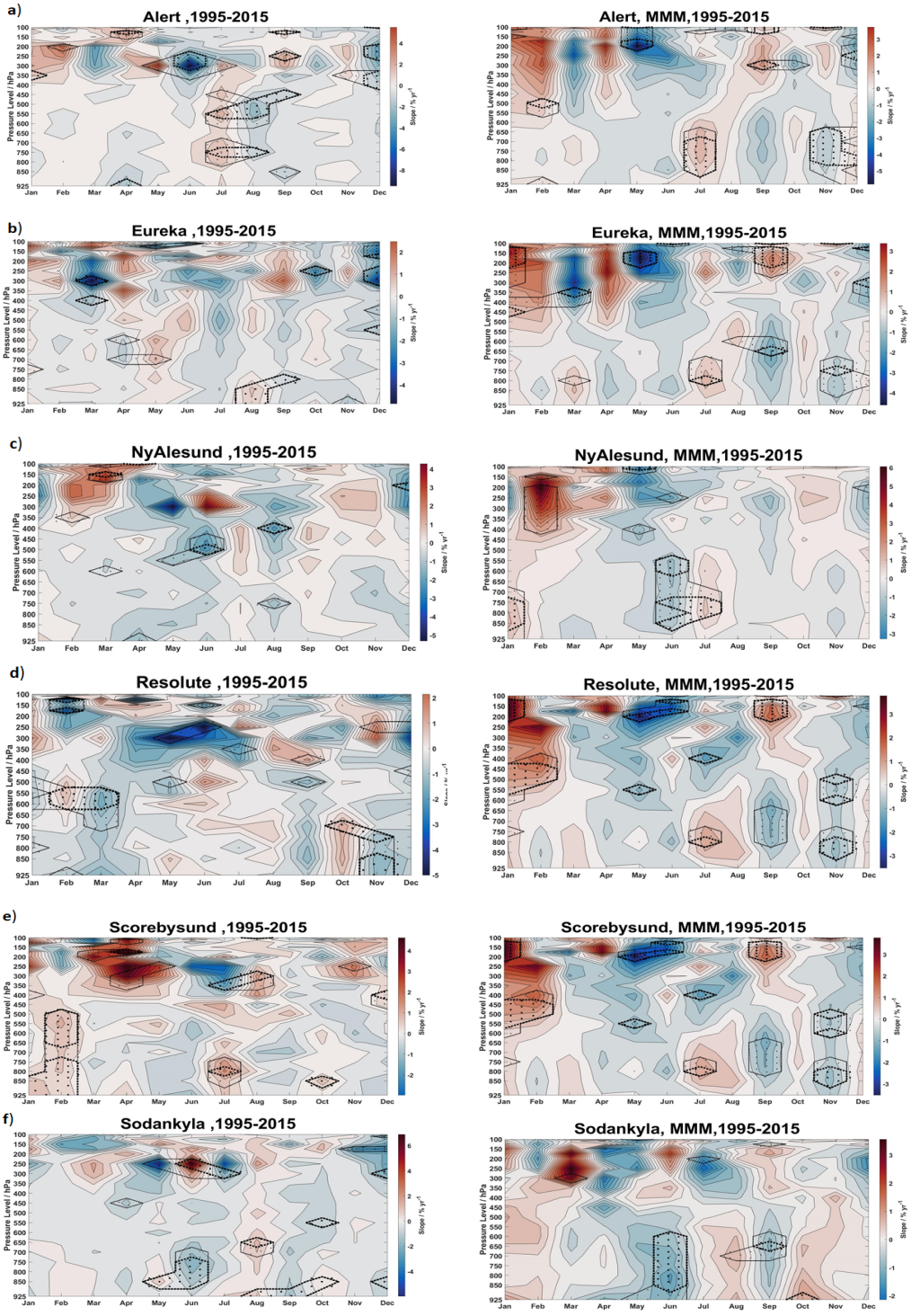

Figure S9: *Comparison of observed (left) and MMM (right) vertical trends in monthly O_3, relative to monthly medians, in % per year, from 925-100 hPa over 1995-2015 at a) Alert, b) Eureka, c) Ny Alesund, d) Resolute, e) Scoresbysund, and f) Sodankyla. Shading/symbols are the same as Fig. S7a.*

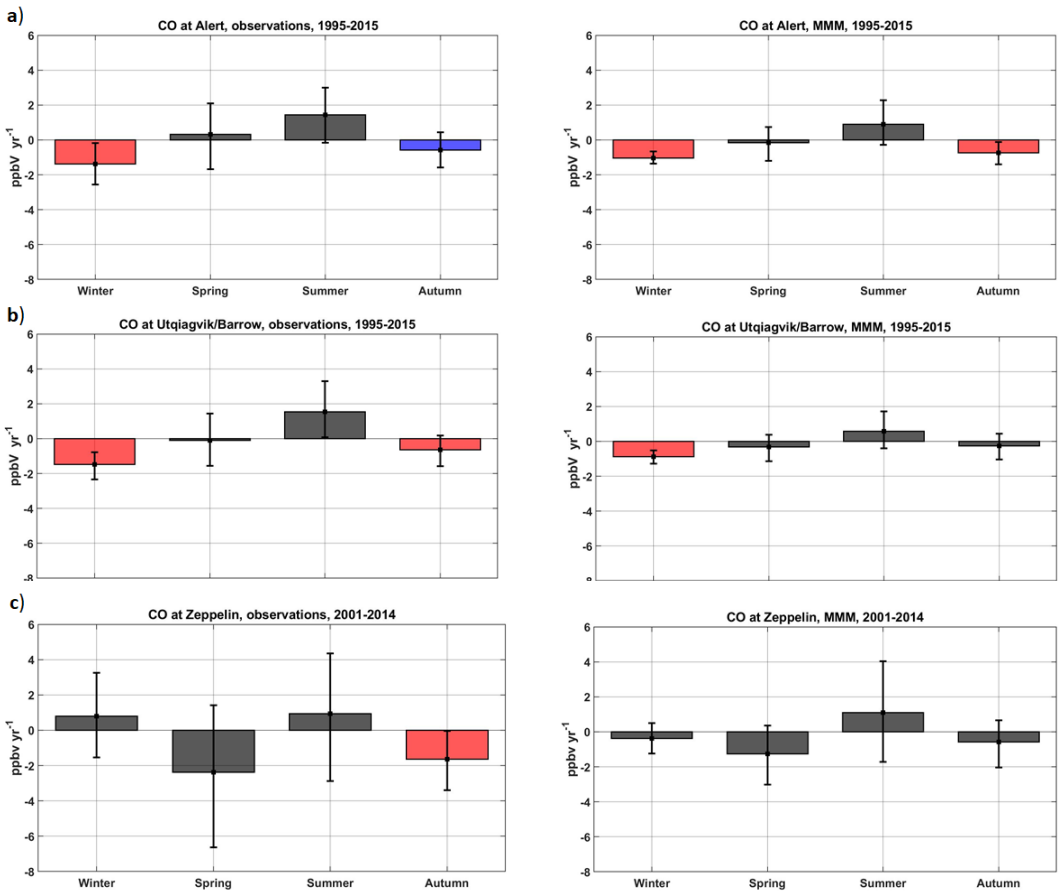

256

257

258 **Figure S10.** *Observed (left) and MMM (right) seasonal surface CO trends at a) Alert, b)*
259 *Utqiagvik, and c) Zeppelin. Boxes represent the slope of the trend in ppbv per year with red boxes*
260 *significant at 95th % CL, blue boxes at 90th % CL, and black boxes not statistically significant.*
261 *Error bars show 95th % CLs.*

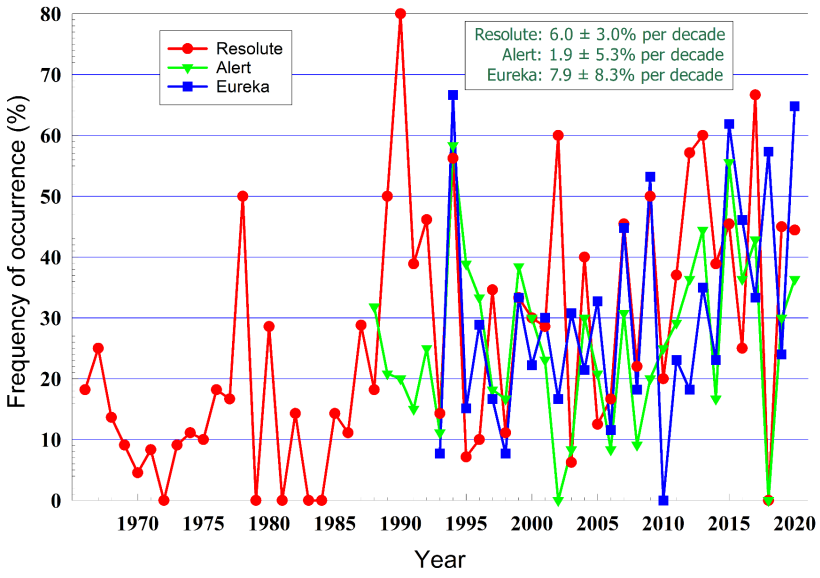

Figure S11. *Frequency of occurrence in % of March to May low O_3 concentrations, defined as <10 ppbv and indicative of O_3 depletion events, using ozonesonde data at the surface, and the first measurement level after balloon release, at Canadian Arctic sites from 1966–2020. Data are adjusted for the effects of occasional variation in sounding frequency. Details about the methodology are given in Tarrasick and Bottenheim (2002).*

Table S1. *Emissions and meteorology used in the models. See Whaley et al. (2022) for further details.*

Model name	**Biogenic emissions**	**Forest fire emissions**	**Meteorology**
CMAM	None	CMIP6	Nudged to ERA-Interim reanalysis
DEHM	MEGANv2	GFAS	Nudged to ERA-Interim reanalysis
EMEP MSC-W	EMEP scheme (Simpson et al., 2012)	FINN (based on Wiedinmyer et al., 2011)	Driven by 3-hourly data from the Integrated Forecast System (IFS) at ECMWF
GISS-E2.1	Isoprene:Guenther et al. (2012); Terpenes: ORCHIDEE; Online DMS, Sea-salt and dust	CMIP6	Nudged to NCEP reanalysis
MRI-ESM2	Biogenic VOCs emissions are taken from Horowitz et al. (2003)	CMIP6	Nudged to the Japanese 55-year Reanalysis (JRA55)
UKESM1	Isoprene and monoterpenes interactive with land surface vegetation scheme	Prescribed from CMIP6 dataset	Nudged to ERA-Interim reanalysis

Table S2. *Annual surface O_3 trends in % per year based at Arctic sites. 'Significance level' is the probability that the observed trend is not the result of random variations. Lower and upper 95 % CLs are also shown together with the significance (confidence) level for the annual trends calculated over the periods indicated. Statistically significant trends (above 90% CL) are in bold. The far right column displays the number of years included in the trend calculation compared to the maximum number of years over the period considered.*

Site	Annual trend (%)	Lower 95% CL	Upper 95% CL	Significance level	Period	Number yrs included/ max. yrs
Alert	**0.29**	0.00	0.75	95%	1999-2019	16/21
	0.24	0.00	0.60	95%	1993-2019	22/27
Utqiagvik	0.53	-0.32	1.18	<90%	1999-2019	20/21
	0.26	-0.21	0.76	<90%	1993-2019	26/27
Villum	**1.98**	0.09	3.11	95%	1999-2019	16/21
	0.68	-0.28	2.30	<90%	1996-2019	18/24
Zeppelin	-0.19	-0.45	0.15	<90%	1999-2019	20/21
	0.18	-0.03	0.46	90%	1993-2019	26/27
Summit	-0.28	-0.77	0.12	<90%	2001-2019	19/19
Esrange	0.08	-0.37	0.64	<90%	1999-2019	21/21
	0.00	-0.24	0.38	<90%	1993-2019	27/27
Pallas	**-0.30**	0.85	-0.06	90%	1999-2019	21/21
	-0.40	-0.84	0.00	90%	1995-2019	25/25
Tustervatn	**-0.52**	-1.14	-0.08	99%	1999-2019	21/21
	-0.18	-0.51	0.08	<90%	1994-2019	26/26

Supplementary Information References:

AMAP. (2015). AMAP Assessment 2015: Black carbon and ozone as Arctic climate forcers. *Arctic Monitoring and Assessment Programme (AMAP)*, 116, ISBN 978-82-7971-092-9. https://www.amap.no/documents/doc/amap-assessment-2015-black-carbon-and-ozone-as-arctic-climate-forcers/1299

AMAP (2021). AMAP Assessment 2021: Impacts of short-lived climate forcers on Arctic climate, air quality, and human health. Arctic Monitoring and Assessment Programme (AMAP), Tromsø, Norway, in press, 2023. Last access 24 January 2023. https://www.amap.no/documents/doc/amap-assessment-2021-impacts-of-short-lived-climate-forcers-on-arctic-climate-air-quality-and-human-health/3614

Collaud Coen, M., Andrews, E., Bigi, A., Martucci, G., Romanens, G., Vogt, F. P. A., and Vuilleumier, L. (2020) Effects of the prewhitening method, the time granularity, and the time segmentation on the Mann–Kendall trend detection and the associated Sen's slope, *Atmospheric Measurement Techniques, 13*, 6945-6964. https://doi/org/10.5194/amt-13-6945-2020

Collaud Coen M. and Vogt F.P.(2008), mannkendall/Matlab: Bug fix: prob_mk_n (v1.1.0). Zenodo. https://doi.org/10.5281/zenodo.4495589

296 Gautrois, M., Brauers, T., Koppmann, R., Rohrer, F., Stein, O., and Rudolph, J. (2003).
297 Seasonal variability and trends of volatile organic compounds in the lower polar
298 troposphere. *Journal of Geophysical Research: Atmospheres*, 108(D13).
299 https://doi.org/10.1029/2002JD002765

300 Gilbert, R. O. (1987) Statistical methods for environmental pollution monitoring, Van
301 Nostrand Reinhold Company, New York. ISBN 0-442-23050-8, 336pp.

302 Guenther, A. B., Jiang, X., Heald, C. L., Sakulyanontvittaya, T., Duhl, T., Emmons, L. K., &
303 Wang, X. (2012). The Model of Emissions of Gases and Aerosols from Nature version 2.1
304 (MEGAN2.1): an extended and updated framework for modeling biogenic emissions.
305 *Geoscientific Model Development*, 5(6), 1471–1492. https://doi.org/10.5194/gmd-5-1471-
306 2012

307 Helmig, D., Petrenko, V., Martinerie, P., Witrant, E., Röckmann, T., Zuiderweg, et al.
308 (2014) Reconstruction of Northern Hemisphere 1950–2010 atmospheric non-methane
309 hydrocarbons, *Atmospheric Chemistry and Physics*, 14, 1463–1483.
310 https://doi.org/10.5194/acp-14-1463-2014

311 Hirsch, R. M., Slack, J. R., and Smith, R. A. (1982) Techniques of trend analysis for
312 monthly water quality data, *Water Resources Research*, 18, 107-121.
313 https://doi.org/10.1029/WR018i001p00107

314 Horowitz, L. W., Walters, S., Mauzerall, D. L., Emmons, L. K., Rasch, P. J., Granier, C., et
315 al. (2003). A global simulation of tropospheric ozone and related tracers: Description and
316 evaluation of MOZART, version 2. *Journal of Geophysical Research: Atmospheres*,
317 108(D24). https://doi.org/10.1029/2002JD002853

318 Kulkarni, A., & von Storch, H. (1995) Monte Carlo experiments on the effect of serial
319 correlation on the Mann-Kendall test of trend, *Meteorologische Zeitschrift, 4(2),* 82-85.
320 https://doi.org/10.1127/metz/4/1992/82

321 Law, K. S., Stohl, A., Quinn, P. K., Brock, C. A., Burkhart, J. F., Paris, J.-D., et al. (2014).
322 Arctic air pollution: New insights from POLARCAT-IPY. *Bulletin of the American*
323 *Meteorological Society*, 95(12), 1873–1895. https://doi.org/10.1175/bams-d-13-00017.1

324 Mackie, A.R., P.I. Palmer, J.M. Barlow, D.P. Finch, P. Novelli and L. Jaeglé (2016)
325 Reduced Arctic air pollution due to decreasing European and North American emissions,
326 *Journal of Geophysical Research-Atmospheres*, 121, 8692-8700.
327 https://doi:10.1002/2016JD024923

328 Marelle, L., Thomas, J. L., Raut, J.-C., Law, K. S., Jalkanen, J.-P., Johansson, L., et al.
329 (2016) Air quality and radiative impacts of Arctic shipping emissions in the summertime in
330 northern Norway: from the local to the regional scale, *Atmospheric Chemistry and Physics,*
331 16, 2359–2379. https://doi.org/10.5194/acp-16-2359-2016

Pernov, J. B., Bossi, R., Lebourgeois, T., Nojgaard, J. K., Holzinger, R., Hjorth, J. L., & Skov, H. (2021). Atmospheric VOC measurements at a High Arctic site: characteristics and source apportionment. *Atmospheric Chemistry and Physics*, 21(4), 2895–2916. https://doi.org/10.5194/acp-21-2895-2021

Salmi, T., Maatta, A., Anttila, P., Ruoho-Airola, T. and Amnell, T. (2002) Detecting trends of annual values of atmospheric pollutants by the Mann-Kendall test and Sen's slope estimates - the Excel template application MAKESENS. *Finnish Meteorological Institute*, 35pp., report FMI-AQ-31, https://www.researchgate.net/publication/259356944

Sen, P. K. (1968), Estimates of the Regression Coefficient Based on Kendall's Tau, *Journal of the American Statistical Association,* 63, 1379-1389. https://doi.org/10.1080/01621459.1968.10480934

Simpson, D., Benedictow, A., Berge, H., Bergström, R., Emberson, L. D., Fagerli, H., et al. (2012). The EMEP MSC-W chemical transport model - technical description. *Atmospheric Chemistry and Physics*, 12(16), 7825–7865. https://doi.org/10.5194/acp-12-7825-2012

Tarasick, D.W., and J.W Bottenheim (2002) Surface ozone depletion episodes in the Arctic and Antarctic from historical ozonesonde records, *Atmospheric Chemistry and Physics, 2*, 197-205, https://doi.org/10.5194/acp-2-197-2002

Theil, H. (1950) A rank-invariant method of linear and polynomial regression analysis, *Proceedings Nederlandse Akademie van Wetenschappen,* 53, 386-392. https://ir.cwi.nl/pub/18446

Walker, T. W., Jones, D. B. A., Parrington, M., Henze, D. K., Murray, L. T., Bottenheim, J. W., et al. (2012). Impacts of midlatitude precursor emissions and local photochemistry on ozone abundances in the Arctic. *Journal of Geophysical Research-Atmospheres*, 117. https://doi.org/10.1029/2011jd016370

Wang, W., Chen, Y., Becker, S., & Liu, B. (2015) Variance correction prewhitening method for trend detection in autocorrelated data, *Journal of Hydrologic Engineering*, 20, 04015033. https://doi:10.1061/(ASCE)HE.1943-5584.0001234

Whaley, C. H., Mahmood, R., von Salzen, K., Winter, B., Eckhardt, S., Arnold, et al. (2022), Model evaluation of short-lived climate forcers for the Arctic Monitoring and Assessment Programme: a multi-species, multi-model study, *Atmospheric Chemistry and Physics, 22*, 5775–5828. https://doi.org/10.5194/acp-22-5775-2022

Whaley, C. H., Law, K. S., Hjorth, J. L., Skov, H., Arnold, S. R., Langner, J., Pernov, et al. (2023), Arctic tropospheric ozone: assessment of current knowledge and model performance. *Atmospheric Chemistry and Physics*, 23, 637-661. https://doi.org/10.5194/acp-23-637-2023

Wiedinmyer, C., Akagi, S. K., Yokelson, R. J., Emmons, L. K., Al-Saadi, J. A., Orlando, J. J., & Soja, A. J. (2011). The Fire INventory from NCAR (FINN): a high resolution global model to estimate the emissions from open burning. *Geoscientific Model Development*, 4(3), 625–641. https://doi.org/10.5194/gmd-4-625-2011

Yue, S., and Wang, C. Y. (2002) Applicability of prewhitening to eliminate the influence of serial correlation on the Mann-Kendall test, *Water Resources Research, 38*, 4-1-4-7, https://doi.org/10.1029/2001WR000861